Pramāṇa, Vol. 20, No. 1, January 1983, pp. 47–54. © Printed in India.

Electron beam fusion, energy compression, and the absolute instability

R JONES
Physics Department, National University of Singapore, Kent Ridge, Republic of Singapore 0511

MS received 8 July 1982; revised 2 November 1982

Abstract. Absolute electron beam-plasma instability is suggested as a means of energy compression for pellet and liner inertial confinement fusion systems.

Keywords. Electron beam; fusion; energy compression; plasma instability.

1. Introduction

Electron beam-plasma instability has been suggested for driving virtually every type of thermonuclear reactor. Because of the excessively large classical mean free path for relativistic electrons in inertial confinement applications Winterberg suggested (Winterburg 1968) that the beam-plasma instability be used to reduce the energy deposition length. Various other means of energy compression or 'densification' (Sahlin 1976) were subsequently described.

Beam-plasma instabilities are of three characteristic types, convective, (Gentle and Lohr 1973), absolute (Carr *et al* 1975) and oscillating (Jones 1977a). The unstable modes lie in distinct bands corresponding to the branches of the plasma dispersion relation (Seidl *et al* 1976) and in the presence of an ambient magnetic guide field the branch situated below the cyclotron frequency is designated the L wave while the upper branch is termed the H wave. L waves may be convective or oscillating only, whereas H waves may be of any of the three basic instability types (Jones 1977b). Similar instabilities arise in the absence of a magnetic beam guiding field.

2. Inertial confinement fusion requirements

Electron beams might be used as drivers for pellet or liner compression fusion systems in one-, two- (figure 1), or three-dimensional geometries. The energy and velocity requirements for such applications can be illustrated by use of a simplified zero-dimensional energy balance model:

$$\frac{1}{T}\frac{\mathrm{d}T}{\mathrm{d}t} = \frac{3(\gamma-1)v}{l} + 2{\cdot}75\times10^{-4} f_\alpha n T^{-5/3} \exp(-211/T^{1/3}) - 3.2\times10^{-14}\frac{n}{T^{1/2}} - \frac{10^{21}}{\ln\Lambda}\frac{T^{5/2}}{nl^2} \quad (1)$$

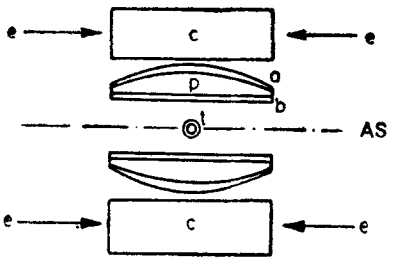

Figure 1. Two dimensional driver: Spherical fusion target, t, or other payload to be compressed by a cylindrically symmetric liner composed of ablator a, pusher p and buffer b. AS is the axis of symmetry and C is a preformed annular plasma heated by electron beams e. An axial magnetic guide field *may* be employed.

where l is the target thickness (in one-and two-dimensional applications) or pellet radius (in three-dimensional geometry) in cm, T is the plasma temperature in eV, n is the plasma density in cm^{-3}, v is the compression speed in cm/sec, $\gamma \approx 5/3$ is the ratio of specific heats, ln Λ is the Coulomb logarithm, and f_α is the fraction of the alpha particle energy absorbed:

$$f_\alpha = \frac{4V/A\lambda_\alpha}{1 + 4V/A\lambda_\alpha)} \tag{2}$$

where V and A are the plasma volume and area, respectively, and λ_α is the range of α particles due to electron energy absorption (Spitzer 1962)

$$\lambda_\alpha = 1{\cdot}38\times 10^{28}\frac{T^{3/2}\,E_\alpha^{1/2}}{n \ln \Lambda} \tag{3}$$

(A 'wetting factor' of 4 was adopted as is the standard practice.) The successive terms in equation (1) account for net plasma temperature rise, compressional heating, alpha particle heating, Bremsstrahlung radiation loss (Boyd and Sanderson 1969) and thermal conduction cooling (Spitzer 1962), respectively (Appendix A).

Equation (1) has been specialized for a three-dimensional compression. For a one-dimensional geometry:

$$\frac{1}{T}\frac{dT}{dt} = \frac{(\gamma-1)\,v}{l} + 2{\cdot}75\times 10^{-4} f_\alpha n\, T^{-5/3} \exp(-211/T^{1/3}) - 3.2\times 10^{-14}\frac{n}{T^{1/2}}$$

$$- \frac{1{\cdot}4\times 10^{21}}{\ln \Lambda}\frac{T^{5/2}}{nl^2}. \tag{4}$$

In our zero-dimensional model only simple numerical factors have changed. A similar relation holds in two-dimensional geometry.

The configuration of figure 1 was presented solely for reasons of simplicity. A better compression (quasi—three-dimensional might be achieved with two cylindrical pushers oriented at 90° to one another in the form of a cross. A set of 3 pushers

arrayed about mutually orthogonal symmetry axes (and with matching coaxial plasmas) might be still better.

The idealized shock kinetics can be approximated by the usual set of Hugoniot relations, for instance in one dimension:

$$n_s = \frac{\gamma + 1}{\gamma - 1} n_0, \tag{5}$$

$$P_s = \frac{2}{\gamma + 1} \frac{n_0 v_s^2}{e}, \tag{6}$$

and

$$v = \frac{\gamma - 1}{2} v_0 = \frac{\gamma - 1}{\gamma + 1} v_s, \tag{7}$$

where v_s and P_s are shock speed and pressure, respectively.

These model equations (in one, two and three dimensions) have been solved in order to determine the energy gain $Q = 1/E \iiint (20 \text{ MeV})\frac{1}{4} n_s^2 \langle \sigma v \rangle \, dx \, dy \, dz \, dt$ and total input energy E as a function of the initial compression or impact speed v_0 (table 1). The results given are approximate but representative and agree with previously published findings (Nuckolls *et al* 1974).

It is widely believed on this basis that compression speeds of $\sim 2 \times 10^7$ cm/sec will be adequate for inertial confinement fusion. Experimentally, power depositions of 10^{13} watt/cm^2 for durations of 3×10^{-9} sec have imparted velocities of 10^7 cm/sec to subscale target foils with $\sim 40\%$ mass ablation. The observed accelerations and energy conversion efficiency were $\sim 8 \times 10^{14}$ cm/sec^2 and 20%, respectively (Ripin *et al* 1980). Such power densities correspond to an ion saturation power flow of:

$$P = 4 \times 10^{-25} n_e (T_e^3/m_i)^{1/2} = 10^{13} \text{ W/cm}^2 \tag{8}$$

from an ablatant plasma of pressure $n_e T_e \lesssim 10^{24}$ eV cm^{-3} (where m_i is the ion mass in grams). If the pellet could be biased then electron saturation power flow might be attainable.

A suitable fusion driver, then, would consist of a 1–10 cm^3 plasma of density $n_e \gtrsim 10^{20}$ cm^{-3}, $T_e \gtrsim 10^4$ eV established in a time $\lesssim 3 \times 10^{-9}$ sec.

Table 1. Energy gain and driver energy as a function of implosion speed.

v_0 (cm/sec) ($\times 10^7$)	One-dimensional		Three-dimensional	
	Q	E(MJ)	Q	E
1	7×10^{-6}	0.2	100	40
2	2×10^{-3}	1.5	100	2
3	3×10^{-3}	5	100	0·4
4	1.5×10^{-1}	14	100	$1{\cdot}4 \times 10^{-3}$
5	7×10^{-1}	30		
6	100	200		
7	100	50		

3. Electron beam-plasma interaction

Classical processes are inadequate for the efficient coupling of relativistic electron beam energy into typical pellet ablatant plasmas (*i.e.* $n_e \sim 10^{20}$ cm^{-3}, $T_e \sim 10^4$ eV, $l \sim 1$ cm) as described in the preceding section. For this purpose beam-plasma instabilities will be considered, either with or without an ambient magnetic field (perhaps required for beam transport).

The simplest relevant linear dispersion relation is that appropriate to a cold weak beam propagating in a cold plasma (Self *et al* 1971)

$$1 - \frac{\omega_{pe}^2}{\omega^2} - \frac{\omega_b^2}{(\omega - kv_b)^2} = 0, \tag{9}$$

where the plasma and beam frequencies are:

$$\omega_{pe}^2 = 4\pi n e^2/m_e, \tag{10}$$

and

$$\omega_b^2 = 4\pi n_b e^2/m_e, \tag{11}$$

with n_b and v_b the beam density and velocity, respectively. The solutions to 9 have a temporal linear growth rate:

$$\delta = \frac{\sqrt{3}}{2}\omega_{pe}(n_b/2n)^{1/3}. \tag{12}$$

No intractable new physics effects result when one includes the relativistic factors (Godfrey *et al* 1975)

$$\omega_b^2 = 4\pi n_b e^2/\gamma^3 m_e, \tag{13}$$

and

$$\delta = \frac{\sqrt{3}}{2}\frac{\omega_{pe}}{\gamma}(n_b/2n)^{1/3}, \tag{14}$$

where

$$\gamma = \left(1 - \frac{v_b^2}{C^2}\right)^{-1/2}. \tag{15}$$

In order to treat the questions of energy deposition and densification one must, however, solve the nonlinear problem (Newton's second law plus the Poisson equation) and consider spatial, rather than temporal growth. Neglecting (for the moment) the relativistic factor we must solve the nonlinear equation set (Carr *et al* 1975 and Seidl *et al* 1976):

$$\pm\frac{dE}{dZ} + \mu_i E = \frac{1}{N}\sum_{n=1}^{N}\sin(2\pi T_n + \varphi), \tag{16}$$

$$\pm E\frac{d\varphi}{dZ} - \mu_r E = \frac{1}{N}\sum_{n=1}^{N}\cos(2\pi T_n + \varphi), \tag{17}$$

$$2\pi \frac{\mathrm{d}^2 T_n}{\mathrm{d}Z^2} = -E \sin(2\pi T_n + \varphi), \tag{18}$$

where
$$\mu_{r,i} = \epsilon_{r,i} (v_0/v_g) \left(\omega_0 \eta \frac{\partial \epsilon}{\partial \omega}\right)^{-1}, \tag{19}$$

$$\eta^3 = (\omega_b^2/\omega_0^2)(v_0/v_g)[(\omega_0/2)(\partial\epsilon/\partial\omega)]^{-1}, \tag{20}$$

and
$$Z = \eta k_0 x. \tag{21}$$

The wave field has the form $E_0 \sin(k_0 x - \omega_0 t + \varphi)$ and is normalized so that the RF power is given by:

$$P_\omega = E^2 (\tfrac{1}{2} m_e v_0^2) n_b \eta \frac{\omega_0}{2} \frac{\partial \epsilon}{\partial \omega} v_b \tag{22}$$

$v_b \approx (\omega_0/k_0)$, and the plasma enters through the wave group velocity v_g and the complex dielectric ϵ_r and ϵ_i.

Integration yields the power balance equation:

$$\tfrac{1}{2}E^2 - \mu_i \int_0^Z E^2 \mathrm{d}Z = -\frac{1}{N} \sum_{n=1}^{N} 2\pi \mathrm{d}T_n/\mathrm{d}Z, \tag{23}$$

which demands that the wave power plus the power dissipated by linear plasma damping equal the beam energy loss rate.

For convective and oscillating instabilities the plus signs are taken in (16) and (17) and the equations are solved using a Newton-Cotes $l=0$, $n=1$ scheme. Typical results are shown in figure 2. The wave profile for oscillating instability is obtained piecewise from the convective solutions using the technique described previously (Jones 1977a, Jones *et al* 1977) assuming a given plasma length L.

To study the absolute instability the minus signs are taken in (16) and (17). The power flow in the wave is toward $Z=0$ so we must impose the condition that $E(Z\to\infty)=0$. This results in an eigenvalue problem in frequency (Carr *et al* 1975 and Seidl *et al* 1976). Typical spatial energy deposition profiles for absolute, convective, and oscillating instabilities are shown in figure 2. The convective wave

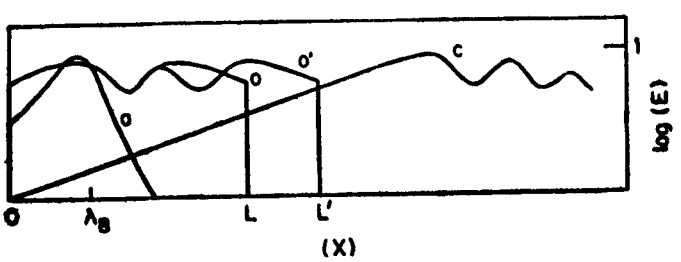

Figure 2. Typical spatial wave energy profiles for absolute instability *a*, convective instability *c* and two oscillating instabilities *O* and *O'* corresponding to plasma lengths *L* and *L'* respectively.

grows up slowly from the point at which the beam enters the plasma ($X=0$) and is unsuitable for heating of very short plasmas. The oscillating instability adjusts its length to that of the plasma (L or L') while the absolute instability has a (short) characteristic length (Seidl *et al* 1976)

$$\lambda_B \approx \frac{2\pi v_b}{\omega_B} \approx \frac{2\pi v_b}{\delta} \approx \frac{2\pi v_b}{\omega_{pe}} (2n/n_b)^{1/3},$$

(where $\omega_B \approx \delta$ at nonlinear wave saturation) or, for relativistic beams:

$$\lambda_B \approx \frac{2\pi C\gamma}{\omega_{pe}} (2n/n_b)^{1/3},$$

Either the absolute or oscillating instabilities (perhaps driven by counterstreaming beams) are capable of heating the small scale ablatant plasmas considered in the previous section. For $n \sim 10^{20}$ cm^{-3}, $\omega_{pe} \sim 6 \times 10^{14}$ sec^{-1}, $\gamma \sim 100$, and $n/n_b \sim 1000$, for instance, $\lambda_B \sim 0.3$ cm. (For large v_b the convective instability is not even excited).

The fractional beam energy deposition is also obtainable (Seidl *et al* 1976) from (16)–(18) (as the change in beam particle kinetic energy) and is typically in the range of $\sim 15\%$. This result has been verified experimentally for low velocity beams (Jones 1977b). Such a figure is poor compared with the 80% absorption efficiency of laser-plasma experiments (Ripin *et al* 1980) but this deficiency is more than offset by (observed) electron beam generator efficiencies of 80–90% as contrasted with comparable laser efficiencies of $\lesssim 5\%$. Under favourable conditions beam modulation (Jones 1977c) and plasma inhomogeneity (Jones 1977d) may also increase the absorption efficiency from $\sim 15\%$ to 25% or more. Beam modulation effects can be understood as a tuning of ω in equations (16)–(18) or a shaping of the ω, k spectrum for optimal growth. Plasma inhomogeneity, on the other hand, modifies the linear dispension relation as a function of z, x in the plasma. Such a modification in the plasma dielectric constant can make the wave phase velocity ω/k a decreasing function of distance along the beam direction z, x. This allows a wave to slow as the beam decelerates, hence maintaining optimal resonance. Ultimately, of course, wave energy must be deposited in plasma particles. An efficient transition to a quasi-linear weakly turbulent state (where the wave energy is small and the plasma particles possess most of the injected energy) is facilitated by multiwave resonances and parametric excitations. With driver dimension > 1 cm (liners, for instance) coupling efficiencies approaching 80% might become possible by taking advantage of wave cascading (Jones *et al* 1976; Jones 1977d).

4. Conclusions

Absolute electron beam-plasma instabilities appear to be an attractive means of energy densification for use in pellet and liner compression fusion. Power densities in excess of 10^{13} watt/cm^2 can be developed with energy deposition efficiencies of at least 15%. Such power levels ($< 10^{14}$ watt/cm^2) are believed to be sufficient for certain inertial confinement fusion schemes (Orens 1980). The convective instabilities assumed by all previous authors are not well suited to these applications.

Acknowledgement

This work was financially supported by NUS Grant RP 36/80.

Appendix A

The zero-dimensional power balance code

Compressional and alpha particle heating are assumed to counter Bremsstrahlung radiation losses and classical thermal conduction cooling. Spitzer (1962) showed that the classical thermal conduction coefficient is:

$$K = \frac{10^{21}\, T^{5/2}}{\ln \Lambda\, n_e} \frac{\text{cm}^2}{\text{sec}}, \tag{A1}$$

where the conduction heat loss is given by:

$$\left.\frac{dT}{dt}\right|_{\text{conduction}} \equiv K \frac{\partial^2 T}{\partial x^2} \to K \frac{T}{l^2}, \tag{A2}$$

or

$$\left.\frac{1}{T}\frac{dT}{dt}\right|_{\text{conduction}} = \frac{10^{21}\, T^{5/2}}{\ln \Lambda\, n l^2}.$$

The alpha particle heating rate is given in terms of a fraction of the fusion reaction rate

$$\left.\frac{d(nT)}{dt}\right|_{\text{fusion alphas}} \equiv \frac{n^2}{4} \langle \sigma v \rangle E_\alpha, \tag{A3}$$

where curve fitting of the reaction rate coefficient has given $\langle \sigma v \rangle \propto T^{-2/3} \exp(-211/T^{1/3})$ in the region of interest. A somewhat simpler approximation,

$$\langle \sigma v \rangle \sim \begin{cases} \alpha T^3, & 6 \text{ keV} \leqslant T \leqslant 10 \text{ keV} \\ \alpha T^2, & 10 \text{ keV} \leqslant T \leqslant 20 \text{ keV} \end{cases}$$

and a more accurate approximation,

$$\langle \sigma v \rangle = 2{\cdot}87 \times 10^{-16} - 8{\cdot}78 \times 10^{-20}\, T + 1{\cdot}02 \times 10^{-23}\, T^2 - 3{\cdot}74 \times 10^{-28}\, T^3 + 4{\cdot}93 \times 10^{-33}\, T^4,$$

have also been employed in typical runs. The fraction of the alpha energy deposited in the plasma f_α is obtained from the ratio of the plasma scale size to the classical

coulomb slowing distance. (This is a pessimistic assumption if fluctuations are present). So:

$$\frac{1}{T}\frac{\mathrm{d}(nT)}{\mathrm{d}t}\bigg|_{\substack{\text{alpha}\\\text{heating}}} = \frac{f_\alpha n \langle \sigma v \rangle E_\alpha}{4T} \approx f_\alpha n E_\alpha T^{-5/3} \exp(-211/T^{1/3}). \quad \text{(A4)}$$

The Bremsstrahlung power loss is given by the usual formula[9] (Boyd and Sanderson 1969)

$$\frac{\mathrm{d}(nT)}{\mathrm{d}t}\bigg|_{\text{Brem.}} = bz^2 n^2 T^{1/2} \quad \text{(A5)}$$

so

$$\frac{1}{T}\frac{\mathrm{d}T}{\mathrm{d}t}\bigg|_{\text{Brem.}} = \frac{bn}{T^{1/2}} \quad \text{(A6)}$$

where $z = 1$.

Compressional heating is assumed to be adiabatic so that the compression ratio $l(t)/l$ (in one dimension) can be related to the temperature rise:

$$\frac{l(t)}{l} = \left(\frac{T_0}{T(t)}\right)^{-\frac{1}{\gamma-1}} \quad \text{(A7)}$$

from which one models the shock heating rate as:

$$\frac{1}{T}\frac{\mathrm{d}T}{\mathrm{d}t} = \frac{(\gamma-1)v}{l}, \quad \text{(A8)}$$

with

$$V = \mathrm{d}l/\mathrm{d}t. \quad \text{(A9)}$$

(Extension to three-dimensions is straightforward.)

Summation of (A2), (A4), (A6) and (A8) yields equation (1).

References

Boyd T J M and Sanderson J J 1969 *Plasma dynamics* (New York: Barnes and Noble) p. 230
Carr W, Jones R and Seidl M 1975 *Plasma Phys.* **17** 623
Gentle K and Lohr J 1973 *Phys. Fluids* **16** 1464
Godfrey B B, Shanahan W R and Thode L E 1975 *Phys. Fluids* **18** 346
Jones R 1977a *Phys. Fluids* **20** 1029
Jones R 1977b *Nuovo Cimento* **B40** 261
Jones R 1977c *Phys. Lett.* **A60** 117
Jones R 1977d *Plasma Phys.* **19** 925
Jones R, Carr W and Seidl M 1976 *Phys. Fluids* **19** 548
Jones R, Carr W and Seidl M 1977 *Phys. Fluids* **20** 791
Nuckolls 1977 European Conference on Laser interaction with matter (Oxford)
Orens J H 1980 in *Naval Res. Lab. Rev.* (July) p. 119
Ripin B H *et al* 1980 *Phys. Fluids* **23** 1012
Sahlin H L 1976 *Energy storage, compression and switching* (New York: Plenum)
Seidl M, Carr W, Boyd D and Jones R 1976 *Phys. Fluids* **19** 78
Spitzer L 1962 *Physics of fully ionized plasmas* (New York: Interscience)
Winterberg F 1968 *Phys. Rev.* **174** 212